Conduction channels and magnetoresistance in polycrystalline manganites

A. de Andrés, M. García-Hernández, and J. L. Martínez
Instituto de Ciencia de Materiales de Madrid (Consejo Superior de Investigaciones Científicas), Cantoblanco, E-28049 Madrid, Spain
(Received 25 January 1999)

We have performed magnetic and transport measurements on several series of $La_{0.7}Ca_{0.3}MnO_3$ polycrystalline pellets and thin films. The aim is to discriminate the effects of structural and chemical disorder on the electronic transport properties of polycrystalline manganites. We propose a macroscopic model that takes into account that electric transport is dominated by the evolution with temperature and external magnetic field of different kinds of parallel connected conduction channels. The relative weight of these channels is determining the overall measured resistance, insulator-to-metal transition temperature, and magnetoresistance. We demonstrate that transport properties of samples with the same magnetic behavior are dominated by the connectivity between grains, but not to grain size effects, at least down to 12 nm grain diameter. The model reproduces very well the magnetoresistance at low temperature for all measured samples with different grain sizes and grain connectivity. [S0163-1829(99)03934-X]

I. INTRODUCTION

Manganese perovskites $La_{1-x}Ca_xMnO_3$ (A=Ca,Sr, Ba . . .) have recently attracted much interest because of their particular transport and magnetic properties. Their high (up to colossal) magnetoresistance (MR) effect[1] make these compounds promising regarding potential magnetic applications. Ca-doped compounds with $0.15<x<0.5$ present an insulator-to-metal transition, at a temperature T_{IM}, tightly related to their para to ferromagnetic transition, at T_c. Both transitions occur at a temperature of about 265 K for the $x=0.3$ compound. The metallic ferromagnetic state is quite well described by the double-exchange model, but polaronic effects due to strong electron-phonon coupling and Jahn-Teller distortions have also to be invoked in the insulator regime, where the conduction is achieved by hopping of small polarons.[2] These effects have also to be taken into account even in compounds that are metallic in the paramagnetic state, as those doped with Sr.

A great deal of interest arose in polycrystalline manganites due to the high magnetoresistance that systems with grain boundaries present at temperatures far from the magnetic transition temperature: Single crystal and epitaxial film magnetoresistance is maximum near T_{IM} ($\simeq T_c$) and almost zero at low temperatures; on the contrary, polycrystalline samples present high magnetoresistance down to low temperatures.[3,4] The effect of grain boundaries, tunnel junctions, and grain size has been extensively studied.[5–7] Several authors report on the decrease of the T_{IM} for polycrystalline systems[8–11] or films with microcracks[12] and related that to grain-size effects,[4,11] or to the presence of insulating regions at grain boundaries.[9] Magnetoresistance due to one single boundary has been evidenced.[13,14] Kim *et al.* suggest that intergranular resistance is probably the origin of the discrepancies between infrared and dc resistivities.[15] Wang *et al.*[16] present the differences in the resistance (with a 300 mT magnetic field and without field) between one sample obtained by conventional sintering and another obtained by ''partial melting'' and relate the differences to ''weak or strong-link grain boundaries.'' Low-field magnetoresistance at low temperature is now established to be a spin-polarized tunneling process at grain boundaries[3,17–19] related to their half metallic character.[20] The description of magnetoresistance in terms of low and high field[11] or intrinsic and extrinsic components[21] attempts to explain the observed behavior.

Nevertheless, several points remain open and some confusion exists with respect to transport data in these systems. While it is well established that the magnetic transition temperature depends on the Mn^{3+} content, that can be altered by different A-site doping or by changing the oxygen stoichiometry,[22] the origin of the differences in the insulator-to-metal transition temperature for samples with the same T_c is unclear. In fact, a model that reproduces the measured resistivity and magnetoresistance as a function of the interfaces and/or grain size, as well as an explanation for the large increase of the magnetoresistance at low temperature for fields above 1 T, when the magnetization is almost saturated, as observed in all polycrystalline manganites, are still lacking.

In the present work we present a simple macroscopic model with very few parameters based on the principles that conduction is mainly achieved through the less resistive channels, which correspond to clean contact areas between grains. It is also assumed that all possible channels are parallel connected. In the first part we demonstrate that electric transport is dominated by the connectivity between the grains. The model reproduces the dependence of the resistance with and without magnetic field (MR) as a function of the temperature as well as the shift or disappearance of the insulator to metal transition. Afterwards we compare the transport data of the pellets to those of polycrystalline thin films. Finally, we show how the low temperature magnetoresistance can be very well reproduced, on the same basis, combining the measured variation of the magnetization with the effect of an applied magnetic field on blocked Mn spins at the grain surface. The external field leads to the opening of new conduction channels parallel connected to those already active at zero field. In summary, this model reproduces the effect of structural and chemical disorder in transport data when the magnetic behavior is the same. We will also dis-

cuss several cases reported in the literature that can be understood taking into account the present model.

II. EXPERIMENTAL DETAILS

Three sets of samples were prepared in order to check the effect of connectivity between grains, grain size, and chemical disorder. Two series of pellets and one series of thin films grown on Si(100) were prepared.

It is well known that La compounds tend to degrade with time when stored in air. We have hints of this degradation by Raman spectroscopy and by the results we present here. The surface of the grains tend to adsorb, probably, CO_2 and H_2O contained in the air. The process is reversible by heating at about 1100 °C, above the temperature of dissociation of lanthanum carbonate (around 800 °C). It is expectable that the smaller the grain size the greater the contamination, because the surface to volume ratio increases as the size of the grains decreases.

Both series of ceramic samples are as follows: One half of $La_{0.7}Ca_{0.3}MnO_3$ powder, with a mean grain size of several microns, is annealed at 1200 °C for 24 h, in order to clean the surface of the grains. The pellets obtained from this powder are labeled C (clean). The other half of the powder was stored in air for several weeks (samples labeled D: dirt surface). With each kind of powder we made four pellets that were sintered at different temperatures; 200, 500, 800, and 1100 °C for 4 h. The number used to label the sample indicates its sintering temperature.

Powder x-ray-diffraction patterns were obtained for all pellets showing identical lattice parameters, shapes, and widths of the diffraction peaks. The size of the grains of the starting powder is in the scale of the micron as observed with an optical microscope. The effect of the sintering treatment is not expected to increase the grain size: the grains of the starting powder are quite large (about 1.5 μm) and the highest sintering temperature was 1100 °C, well below the melting point (above 1600 °C). Therefore, the sintering effect can only be to glue one grain to the other. In order to increase the size of the grains, it would be necessary to rotate the grains so as to align the crystallographic axes of two or more grains. This process has certainly not taken place in our samples due to the large starting grain size and ''low'' sintering temperatures. SEM microphotographs of three of the pellets (C200, C800, and D1100) have been taken. The images show that the mean grain size is identical for the three samples, and can be estimated to be about 1.5 μm. We can ascertain that all the pellets have the same mean crystalline grain size. The connectivity between grains will depend on the sintering temperature while the quality of the grain surface depends on the starting powder (clean or dirty grains).

The effect of the grain size is checked by comparing these ceramic samples to a series of polycrystalline thin films of different grain sizes. The thin films were grown by dc sputtering at room temperature on Si (100) substrates in a mixed Ar and O_2 atmosphere (ratio 4:1) and then annealed at 850 °C for 600 s. The films atomic-force microscopy images show grains of rather spherical shape with mean diameters between 12 and 80 nm depending on film thickness (between 100 and 1200 nm). Grazing incidence and standard x-ray diffraction of the thin films revealed their polycrystalline

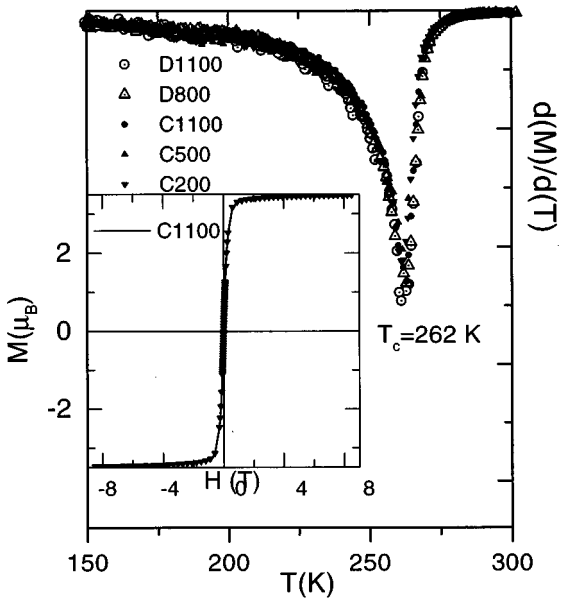

FIG. 1. Derivative of the magnetization at 1000 Oe of several representative pellets. Inset: hysteresis cycles of two pellets. The samples are labeled with a letter (D is the dirt surface, C is the clean surface), and a number, which is the sintering temperature of the pellet.

character and expected lattice parameters for Ca concentration of about 28%. The details of the growth, structure, morphology, and transport properties have been presented elsewhere.[23]

The magnetization measurements were performed either in a superconducting quantum interference device magnetometer (for the thin films) or in a physical properties measurement system (PPMS) from Quantum Design (pellets). The transport measurements were all performed in the PPMS with a standard four-probe configuration.

III. RESULTS AND DISCUSSION

First of all, magnetic and transport behavior of both series of pellets, with the same grain size, are presented. Figure 1 shows the magnetic behavior of several representative pellets. The magnetic transition temperature is identical for all of them and, at 5 K, the magnetization is practically saturated at about 1 T (see inset). Figures 2(a) and 2(b) present the resistance of the same samples, measured at 0 and 9 T, normalized by their respective values at 300 K and 0 T. The arrows indicate the maximum in the resistance corresponding, in principle, to the insulator-to-metal transition. Notice that the D200 sample does not even show a metallic regime. The magnetic transition temperature (T_c) is also indicated. It can easily be observed in Fig. 2 that, as the sintering temperature decreases, the insulator-to-metal transition temperature (T_{IM}) decreases and $R(T)/R(300\ \mathrm{K})$ dramatically increases at low temperatures. Moreover, the resistance at 300 K increases several orders of magnitude (not seen in Fig. 2 because data are normalized to $R(300\ \mathrm{K}, 0\ \mathrm{T})$. A similar dependence of the resistance with temperature as that presented by samples sintered between 200 and 800 °C have been reported for thin films and powder samples with small grain size, obtained by sol-gel techniques, and either have

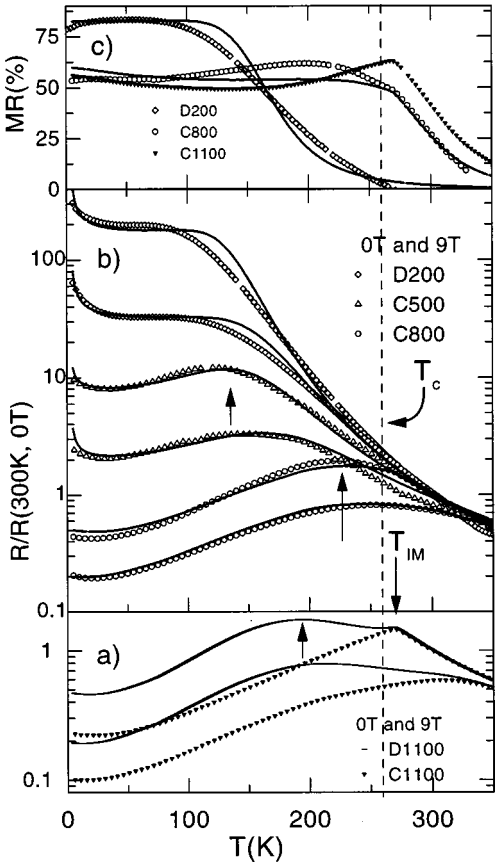

FIG. 2. Normalized resistance at 0 and 9 T for (a) two pellets, both annealed at 1100 °C but with clean (C1100) and dirt (D1100) starting powders showing the effect of a dirt surface in the resistance and (b) pellets annealed at different temperatures (200, 500, 800, and 1100 °C). (c) Magnetoresistance for three samples. Continuous lines are the fits detailed in the text.

been related to grain-size effects or have been overlooked. We will comment on this point later, but in the present series of samples we do not have different oxygen content, except in the contaminated D samples where the composition of the surface layer of the grains is not known. Nevertheless, because the magnetic transition temperature is identical for all pellets, even for the dirt samples, the average oxygen content is expected to be very nearly the nominal one.

We propose the following phenomenological model that can explain the large differences in the measured electric resistance, $R(T)$, taking into account that magnetic properties are identical for all pellets: Two kinds of conduction channels are present in the samples and all of them are parallel. One kind is related to the intrinsic transport properties of the system and is achieved through good contacts between grains. The other kind of channels show energy barriers that inhibit metallic conduction at all temperatures due to poor connectivity, disorder, and/or contamination. These defects are mainly due to the fact that there are physical barriers between grains because (i) the grains are not close enough, (ii) their surface is contaminated, (iii) Mn environment at the surface is not the same as that inside the grains; in all cases Mn-O-Mn paths can be broken or distorted decreasing the conductivity. The actual situation is probably very complicated with a large distribution of barriers but, in fact, from the conduction point of view, it is not so important: among

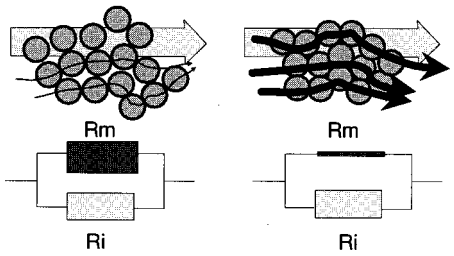

FIG. 3. Schema for the conduction in two granular systems with a poor connectivity (left) and a better connectivity (right). Lower part: the equivalent circuits with two resistances in parallel: R_M (for good channels) and R_I (for bad channels). The curved arrows in the upper part are related to good channels.

the different channels, the conduction will be effected through the less resistive ones because these are parallel channels. Moreover, as the temperature decreases, the available thermal energy to overcome the barriers decreases exponentially so the contribution to the conductivity of ''bad channels'' decreases accordingly. On the other hand, depending on the connectivity of the grains, which is determined by the sintering temperature, and on the quality of the surface, the effective section for ''good'' conduction, with respect to that of other paths, changes from one sample to another. Figure 3 illustrates this picture for electric transport. For the present samples the effect of ''contamination'' is less important than connectivity since $R(T)$ curves are very similar for pellets sintered at the same temperature, for example D200 and C200, or D500 and C500. Only the best sintered samples (at 1100 °C) present a clear difference in their resistance curves [Fig. 2(a)]: the metal-transition temperature changes from 270 to 190 K (for C1100 and D1100, respectively). This means that conduction barriers due to bad physical contacts between grains are higher than those related to a contaminated surface. Obviously, if the surfaces of the grains are more degraded than in the present samples, its effect can be more important, as it can be the case for samples with very small grain size obtained from ball milling or sol-gel techniques. In any case both kinds of defects play, qualitatively, the same role, and have to be very carefully considered before trying to extract conclusions from resistance data, especially when the magnetic transition temperature of the samples are identical. Electric transport data can be dominated by this kind of spurious effect.

This model can also be applied to Sr-doped manganites which are nominally metallic above T_c and where bad connectivity and/or contamination of the grain surface can lead to an apparent semiconductor behavior and to an increase of the resistance, depending on the relation of the sections for ''good'' and ''bad'' channels. The explanation is valid also for polycrystalline films with the same T_c but different oxygen content: the T_c value is related to the composition of the major part of the film, nevertheless small variation of the oxygen content, localized at the grain surface will break the Mn-O-Mn channels from one grain to the other increasing the measured resistance.

Xiong *et al.*[24] have reported the resistivity curves for several epitaxial $Nd_{0.7}Sr_{0.3}MnO_3$ films prepared changing the oxygen pressure during the deposition. The data show that, depending on the sample, the peak temperature (at which the

resistance is maximum) varies from 170 down to 50 K, or even lower. The authors propose that the films can be seen as a paramagnetic matrix paralleled by ferromagnetic filamentary paths, but they do not relate the transport changes to any characteristic of the films. True epitaxial films with the correct composition present a single-crystal behavior, so we propose, in this case, that it is very probably related to a variation in the oxygen content of the films. This can be easily checked because T_c would change from one film to another depending on the oxygen content, disappointingly, the authors do not give the magnetic transition temperatures for the different films.

We show now that this model, with only two parameters, can quantitatively very well reproduce the dependence of the resistance with temperature, with and without external magnetic field, of all pellets. In the present case, above T_c, the lowest barrier for conduction is that of polaron hopping from one Mn to another, which is about 100 meV.[25] For the present samples we have fit the paramagnetic phase data to a semiconductor model obtaining an activation energy about this value for all samples. The fit to a polaronic conduction mechanism leads to a slightly different activation energy but identical quality of the fit in the measured temperature range (up to 350 K). In fact, it is necessary to considerably enlarge the temperature range (towards high temperatures) to be able to discern between both conduction processes (thermally activated carriers or polaron hopping).

We model the measured resistance as two resistances in parallel: $1/R=(S_m/\rho_m+S_i/\rho_i)$ with resistivities ρ_m (for good channels which are metallic below T_c) and ρ_i (bad channels: always insulating, with an activation energy E_i) with effective sections S_m and S_i, respectively (we consider always the unit length). The resistivity of ''good channels'' (ρ_m) should be that of a good quality single crystal, but we do not have such a crystal, therefore, we take $\rho_m(T)=\rho(C1100,T)+A\exp(E_a/k_BT)$ i.e., the resistivity of our best sample, in series with a component that takes into account the low temperature (below 50 K) increase of the resistance. This rise of the resistance is often observed and has been related to the Coulomb blockade. This is probably the process for very small grains but in the present case (as for many of the reported in the literature) we associate this contribution with small structural distortions at grain boundaries, that give rise to small activation barriers E_a and which are observable only at low temperature where the ''intrinsic'' metallic resistivity is very low. This contribution to $\rho_m(T)$ is modulated by an amplitude factor A and we take $E_a=5$ K $=0.43$ meV for all samples. The insulating paths are simply modeled by a semiconductorlike resistivity: $\exp(E_i/k_BT)$ with $E_i=100$ meV (the paramagnetic phase activation energy).

Continuous lines in Fig. 2(b) are the fits for several samples at 0 and 9 T with this simple model, where the only parameters are S_m/S_i and A. The activation energies (E_i and E_a) being the same for all samples. In order to fit the 9 T measured resistance it is necessary to increase S_m: as we shall see later, the external magnetic field increases the effective section for the good channels. The values for the fitting parameters are collected in Table I. It can therefore be concluded that (i) the observed phenomenology can be very well understood with two kinds of parallel paths, (ii) it is independent of the grain size or of the width of the claimed grain shell. In turn, it depends on the fraction of the sample with good conduction.

TABLE I. Parameters of the fits to resistance data presented in Fig. 2. S_m/S_i is the ratio of the effective sections for ''good'' and ''bad'' conduction channels. A is the weight of the low-temperature component to resistance.

Sample	Magnetic field	S_m/S_i	A
C800	0 T	0.833	0
	9 T	1	0
D500	0 T	0.0435	0.1
	9 T	0.111	0.1
D200	0 T	0.0125	1.8
	9 T	0.0666	1.8

An early experiment,[26] that, in our opinion, supports this model, presents the differences between dc and microwave resistivities in polycrystalline $Nd_{0.7}Sr_{0.3}MnO_3$. While dc resistivity shows a slow decrease below T_c and a relatively high residual resistance at low temperature, the resistivity obtained from microwave (10 GHz) absorption shows a single-crystal-like behavior: steep decrease below T_c and low resistivity at low temperature. The single-crystal-like behavior can be understood taking into account that, at so high frequencies, the major part of the carriers cannot cross the boundaries from grain to grain, therefore the resistivity is that of each grain which is, obviously, a small single crystal. Very tightly related to these experiments are the comparison of dc resistivity measurements to the conductivity extracted from the far-infrared reflectivity at low temperatures, in the metallic phase.[15] The dc resistivity is higher than that obtained from the free-carrier density, because in the first case the carriers have to cross the grain boundaries so the measured resistance depends on the fraction of the sample with good conduction. In fact, at low temperature, where the conduction is effective basically only through good contacts, the resistivity ($\rho=R.S/l$) obtained from the measured resistance (R) and herein called the S_m section, instead of that of the whole sample, would be very similar to the values obtained from microwave or infrared experiments. This point is to stress that, in many cases, the resistivity obtained from the resistance and the geometrical parameters of the sample and the experiment is not describing an intrinsic property of the samples, as it can be dominated by the quality of the sintering process. Recently, an interesting experiment has been reported[12] on artificially induced microcracks in epitaxial films. The authors report a large increase of the ''resistivity'' and decrease of the insulator-to-metal transition temperature for films with cracks compared to those without cracks, all of them with the same magnetic transition temperature. This behavior, again, can be explained with the present model: the microcracks change the connectivity, i.e., the section for good channels.

Figure 2(c) presents the measured and calculated magnetoresistance for D200 and C800 samples together with measured MR for C1100 as a function of temperature. Note that only by changing the relative weight of ''good'' and ''bad'' channels we can reproduce the enormous observed changes in the shape of the magnetoresistance: As the connectivity

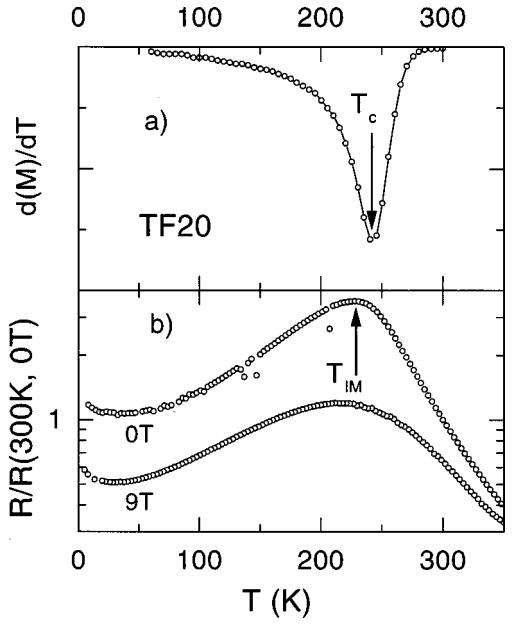

FIG. 4. (a) Derivative of the magnetization at 1000 Oe and (b) resistance at 0 and 9 T of a thin film with 20 nm grains (TF20).

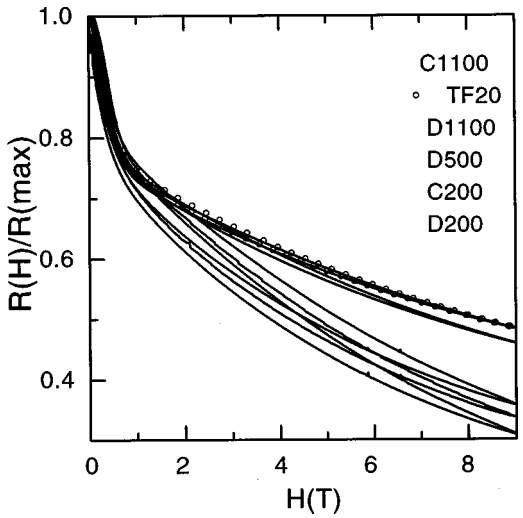

FIG. 5. Magnetoresistance at 5 K of several pellets and a representative thin film (TF20). The labeling of the pellets is explained in Fig. 1 caption.

decreases the magnetoresistance decreases near T_c and increases at low temperature. Therefore, grain boundaries are the origin of the differences between the single crystal and polycrystal behavior in two ways. This point is evidenced by the variation of the resistance at low temperature (when the thermal activation of the carriers is very much limited) with the applied magnetic field. At low fields, up to the nearly fully magnetization of the sample, the principal process in electronic transport is the spin-polarized tunneling at grain boundaries. Simultaneously, the progressive ordering of some Mn blocked spins at the grain surface opens new channels in parallel, which decrease more and more the resistance.

In order to demonstrate that the observed behavior in the resistance is not due to grain-size effects, we present magnetic and transport data for thin films with very small grain size, down to 12 nm, all of them with the same T_c and T_{IM}. Figure 4 shows data for a representative thin film (T_c $=242$ K) with grains of about 20 nm. T_{IM} and T_c are nearly identical indicating the good quality of the samples and a good connectivity. In fact magnetoresistance at 5K [or equivalently $R(H)/R(0)$] of C1100 and the thin film (TF20) are identical (Fig. 5). The slope of the high-field magnetoresistance at 5 K reported for different manganites with grain sizes above 500 nm are all nearly identical (around 0.23) and coincides with our data for the C1100 sample and for all our thin films (grain diameters between 80 and 12 nm).

In Fig. 5 we present the measured $R(H)/R(0)$ at 5 K for several pellets and a representative thin film (in particular with mean grain size of 20 nm). It is readily observed that magnetoresistance of the TF20 thin film and C1100 pellet are identical, while pellets with worse connectivity and/or contaminated grain surface have a higher slope of $R(H)/R(0)$ in the high-field region.

It is important to stress that there can be grain-size effects in the transport properties, as is the case, and, in principle, these should be related to differences in the magnetic behavior. For example, our thin films present a higher coercive field than the pellets, and their magnetic transition is less sharp, as observed comparing Figs. 1 and 2, these are, very probably, grain-size effects. Moreover, the low-field MR, which is related to a different behavior of the magnetization $[M(H)]$, is also dependent on the grain size. However, one of our main points in this paper is to underline that other effects, apart from grain size, can take place and, in fact, can be dominating the electric transport.

Figure 6 shows C1100, D200, and TF20 measured magnetoresistance together with a fit considering the following mechanism: At low temperature the good channels give rise to a magnetoresistance which is determined by the spin-polarized tunneling between grains that depends on the angle formed by the magnetic moments of these grains.[20] The variation of this angle with the external magnetic field is given by the measured magnetization $M(H)$. Therefore, the

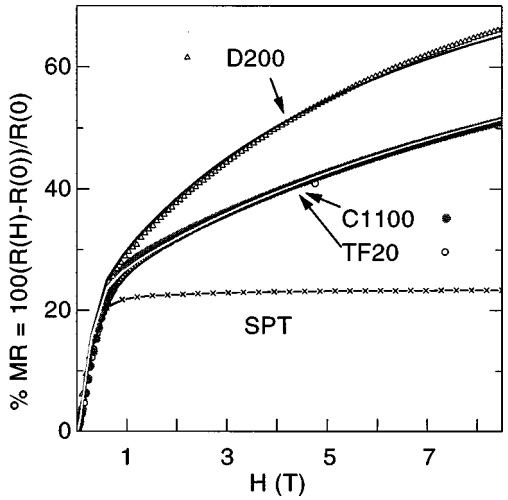

FIG. 6. Magnetoresistance of C1100 and D200 pellets and TF20 thin film (gray symbols). Crosses are the magnetoresistance obtained from the measured magnetization of a pellet (inset of Fig. 1) and continuous lines (black and white) are the fits to the magnetoresistance of three samples.

conductivity for good channels σ_G can be described by the following expression:

$$\sigma_G(H) = \sigma_G(0) + C[(M(H)/M_s]^2,$$

where M_s is the saturated magnetization and C is a constant for a given temperature, and

$$R_G(H)/R_G(0) = 1/(1 + C[(M(H)/M_s)^2/\sigma_G(0)].$$

The related magnetoresistance, defined as $MR(H) = 100[R_G(H)/R_G(0) - 1]$, is represented by crosses in Fig. 6. At the grain surface Mn spins can be blocked because, for example, their environment is unbalanced or because of magnetic anisotropy. In fact recent calculations demonstrate that Mn ions of the outmost layer have their e_g orbitals split, their charge state modified, and a tendency to order antiferromagnetically.[27] Magnetic measurements can be insensitive to these disordered Mn spins, because the fraction is very small, but the conduction at low temperature is drastically reduced because one distorted Mn can close this conduction channel. The hypothesis of this model is that the magnetic field (H) aligns Mn spins blocked at the surface in a linear way opening new conduction channels. The effective section for electric conduction is $S_{\text{new}}(H) = f \cdot H$, where f is a constant. As these are parallel channels the inverse of the resistances are added and we obtain

$$R(H)/R(0) = 1/[1 + (C/\sigma_G(0))(M(H)/M_s)^2][1 + f \cdot H/S_G],$$

where S_G, the good section for conduction at $H = 0$, depends on the connectivity and contamination of the sample. In the fits in Fig. 6: $C/S_G(0) = 0.33$ (for the three samples) and $f/S_G = 0.068$ (for the C1100 and TF20 samples) and 0.14 (for the D200 sample), which is consistent with the idea that the effective section for good conduction (S_G) of sample C1100 is larger than that for D200. Note that high-field magnetoresistance is not linear and that this model fits perfectly the data in the whole measured magnetic field range for all samples with only one parameter (f/S_G).

IV. CONCLUSIONS

In the present paper we have shown that the interpretation of transport data has to be very carefully done. A T_{IM} considerably lower than T_c together with a high resistivity at low temperature is an indication of bad connectivity between grains and not a grain-size effect. It has to be taken into account that the conduction is achieved by parallel channels and that the resistivity of these channels vary in a different way with temperature depending on whether the metallic regime is reached or not. The section for metallic conduction is determined by the connectivity between grains that depends on how good is the sintering and/or the contamination of the grain surface. The effect of an external magnetic field is to align blocked spins at the surface of the grains in a linear way opening new conduction channels. Mn ions at the surface can block the conduction if their e_g levels are split introducing an activation barrier therefore increasing drastically the resistance as temperature decreases. This model is valid for all granular systems whose main transport mechanism is spin-polarized tunneling.

ACKNOWLEDGMENTS

We thank L. Brey and F. Guinea for fruitful discussions, L. Vazquez for AFM measurements, and J.M. Alonso for preparing manganite powder. This work was supported by CICyT under Contract Nos. MAT96-0395 and MAT97-725.

[1] S. Jin, T. H. Tiefel, M. MacCormack, R. A. Fastnacht, R. Ramesh, and L. H. Chen, Science **264**, 413 (1994).
[2] M. R. Ibarra and J. M. de Teresa, in *Giant Magnetoresistance and Related Properties of Metal Oxides*, edited by C. N. R. Rao and B. Raveau (World Scientific, Singapore, in press).
[3] H. Y. Hwang, S. W. Cheong, N. P. Ong, and B. Batlogg, Phys. Rev. Lett. **77**, 2041 (1996).
[4] A. Gupta, G. Q. Gong, G. Xiao, P. R. Duncombe, P. Lecoeur, P. Trouilloud, Y. Y. Wang, V. P. Dravid, and J. Z. Sun, Phys. Rev. B **54**, 15 629 (1996).
[5] Y. Lu, X. W. Li, G. Q. Gong, G. Xiao, A. Gupta, P. Lecoeur, J. Z. P. Sun, Y. Y. Wang, and V. P. Dravid, Phys. Rev. B **54**, 8357 (1996).
[6] M. Viret, M. Drouet, J. Nassar, J. P. Contour, C. Fermon, and A. Fert, Europhys. Lett. **5**, 545 (1997).
[7] P. Lyu, D. Y. Xing, and J. M. Dong, Phys. Rev. B **58**, 54 (1998).
[8] R. Ramesh, R. Mahendiran, A. K. Raychaudhuri, and C. N. R. Rao, Appl. Phys. Lett. **68**, 2291 (1996).
[9] S. Pignard, H. Vincent, J. P. Senateur, K. Frohlich, and J. Souc, Appl. Phys. Lett. **73**, 999 (1998).
[10] R. D. Sánchez, J. Rivas, C. Vázquez-Vázquez, A. López-Quintela, M. T. Causa, M. Tovar, and S. Oseroff, Appl. Phys. Lett. **68**, 134 (1996).
[11] Ll. Balcells, J. Fontcuberta, B. Martínez, and X. Obradors, Phys. Rev. B **58**, 14 697 (1998).
[12] K. M. Satyalakshmi, B. Fisher, L. Patlagan, G. Koren, E. Sheriff, R. Prozorov, and Y. Yeshurun, Appl. Phys. Lett. **73**, 402 (1998).
[13] K. Steenbeck, T. Eick, K. Kirsch, K. Odonnell, and E. Steinbeiss, Appl. Phys. Lett. **71**, 968 (1997).
[14] N. D. Mathur, G. Burnell, S. P. Isaac, T. J. Jackson, B. S. Teo, J. L. Mac Manusdriscoll, L. F. Cohen, J. E. Evetts, and M. G. Blamire, Nature (London) **387**, 266 (1997).
[15] K. H. Kim, J. Y. Gu, H. S. Choi, D. J. Eom, J. H. Jung, and T. W. Noh, Phys. Rev. B **55**, 4023 (1997).
[16] X. L. Wang, S. X. Dou, H. K. Liu, M. Ionescu, and B. Zeimetz, Appl. Phys. Lett. **73**, 396 (1998).
[17] X. W. Li, A. Gupta, G. Xiao, and G. Q. Gong, Appl. Phys. Lett. **71**, 1124 (1997).
[18] R. Shreekala, M. Rajeswari, K. Ghosh, A. Goyal, J. Y. Gu, C. Kwon, Z. Trajanovic, T. Boettcher, R. L. Greene, R. Ramesh, and T. Venkatesan, Appl. Phys. Lett. **71**, 282 (1997).
[19] J. M. D. Coey, Philos. Trans. R. Soc. London, Ser. A **356**, 1539 (1998).
[20] J. H. Park, E. Vescovo, H. J. Kim, C. Kwon, R. Ramesh, and I. Veukatesan, Nature (London) **392**, 794 (1998).
[21] P. Raychaudhuri, K. Sheshadri, P. Taneja, S. Bandyopaghyay, P. Ayyub, A. K. Nigam, and R. Pinto, Phys. Rev. B **59**, 13 919 (1999).
[22] H. L. Ju, J. Gopalakrishnan, J. L. Peng, Qi Li, G. C. Xiong, T.

Venkatesan, and R. L. Greene, Phys. Rev. B **51**, 6143 (1995).
[23] M. García-Hernández, J. L. Martínez, A. de Andrés, L. Vázquez, E. Herrero, and J. M. Alonso, J. Magn. Magn. Mater. **196-197,** 530 (1999).
[24] G. C. Xiong, S. M. Bhagat, Q. Li, M. Domínguez, H. L. Ju, R. L. Greene, T. Venkatesan, J. M. Byers, and M. Rubinstein, Solid State Commun. **97**, 599 (1996).
[25] I. O. Troyanchuk, Zh. Éksp. Teor. Fiz. **102**, 251 (1992) [Sov. Phys. JETP **75**, 132 (1992)].
[26] M. Domínguez, S. M. Bhagat, S. E. Lofland, J. S. Ramachandran, G. C. Xiong, H. L. Ju, T. Venkatesan, and R. L. Greene, Europhys. Lett. **32**, 349 (1995).
[27] M. J. Calderón, L. Brey, and F. Guinea, Phys. Rev. B **60**, 6698 (1999).